JOURNAL OF THE KOREAN ASTRONOMICAL SOCIETY
29: 171~179, 1996

JK INFRARED PHOTOMETRY OF THE GLOBULAR CLUSTER M3

LEE, SANG-GAK, LEE, MYUNG GYOON AND KIM, EUNHYEUK
Department of Astronomy, Seoul National University
E-mail : sanggak@astrosp.snu.ac.kr,mglee@astrog.snu.ac.kr,ekim@astro.snu.ac.kr
(Received September 25, 1996; Accepted October 15, 1996)

ABSTRACT

We have obtained the JK images of the central region of the globular cluster M3 (NGC5272), using the 256×256 InSb array. We present JK photometry of bright red giant branch stars in the central $2'.2\times2'.2$ region of M3. The infrared color-magnitude diagrams are presented. The comparison of the red giant branch of M3 with that of M13 confirms that both globular clusters have similar metal abundances.

Key Words: JK infrared photometry, globular cluster, M3

I. INTRODUCTION

M3 is one of the brightest northern globular cluster, of which the first optical photometric study was done by Sandage (1953) more than 40 years ago . The subsequent photometric studies in the optical band have been carried out by Sandage(1970), Sandage and Katem (1982), Auriere and Cordoni(1983), Buonanno *et al.* (1986, 1989, 1994). Later deep CCD photometry of M3 has been presented by Paez, Roger, & Straniero(1990) and Paez, Straniero, & Roger(1990). Recently some photometric studies with the Wide Field Planetary Camera of the Hubble Space Telescope have been carried out by Guhathakurta *et al.* (1994) and Burgarella *et al.* (1995).

Because of its brightness, proximity, and location at high galactic latitude, morphologies as well as fundamental parameters of M3 are fairly accurately known so that M3 can used as a prototype globular cluster of poor metallicity. Also the stellar populations of M3 have been a powerful testbench for the population synthesis for cosmological purposes as well as for the predictions of the stellar evolution theory.

Although a lot of studies on this globular cluster have been carried out and this cluster has been used as a yard stick to derive other clusters's properties, not many works on infrared photometry have been done. Some near-infrared photoelectric photometry works on individual stars in M3 were presented by Cohen *et al.* (1978), Phillips *et al.* (1986), Frogel *et al.* (1983), and Arribas & Martinez Roger (1987), and a preliminary result on JK photometry of M3 based on the InSb array camera imaging was presented by Guarnieri *et al.* (1990).

The introduction of the large-format near-infrared detector arrays makes photometric surveys feasible at wavelength longer than 1 μm. Taking the advantage of low interstellar reddening of near-infrared over optical region, most near-infrared studies for globular clusters in the recent past were concentrated to those in low Galactic latitudes (Davidge & Simons 1994; Davidge & Harris 1995) and those in the Galactic bulge (Davidge & Harris 1996; Davidge *et al.* 1996).

However, M3 can be an excellent comparison cluster for metal-poor clusters. M3 is commonly believed to be a cluster quite unaffected by reddening. Most of the determinations of this parameter agree on $E(B-V)=0.00\sim0.01$ (Burstein & McDonald 1975; Bica & Pastoriza 1983; Paez *et al.* 1990). If the selective extinctions of $A_J = 0.28A_V$ and $A_K = 0.11A_V$ (Rieke & Lebofsky 1985) are adopted, the extinction of M3 is negligible at J, H, and K bands. This is the reason we need a near-infrared photometric study on M3.

In order to investigate the near infrared photometric properties of stars in M3, we have obtained J and K images around the center of this cluster. We present JK photometry of the bright red giant stars in the central region of M3 in this paper. Observations and data reduction are described in Section II. The morphologies of the resulting color-magnitude diagrams are discussed in Section III, and the comparisons of the CMDs of M3 and M13 are presented

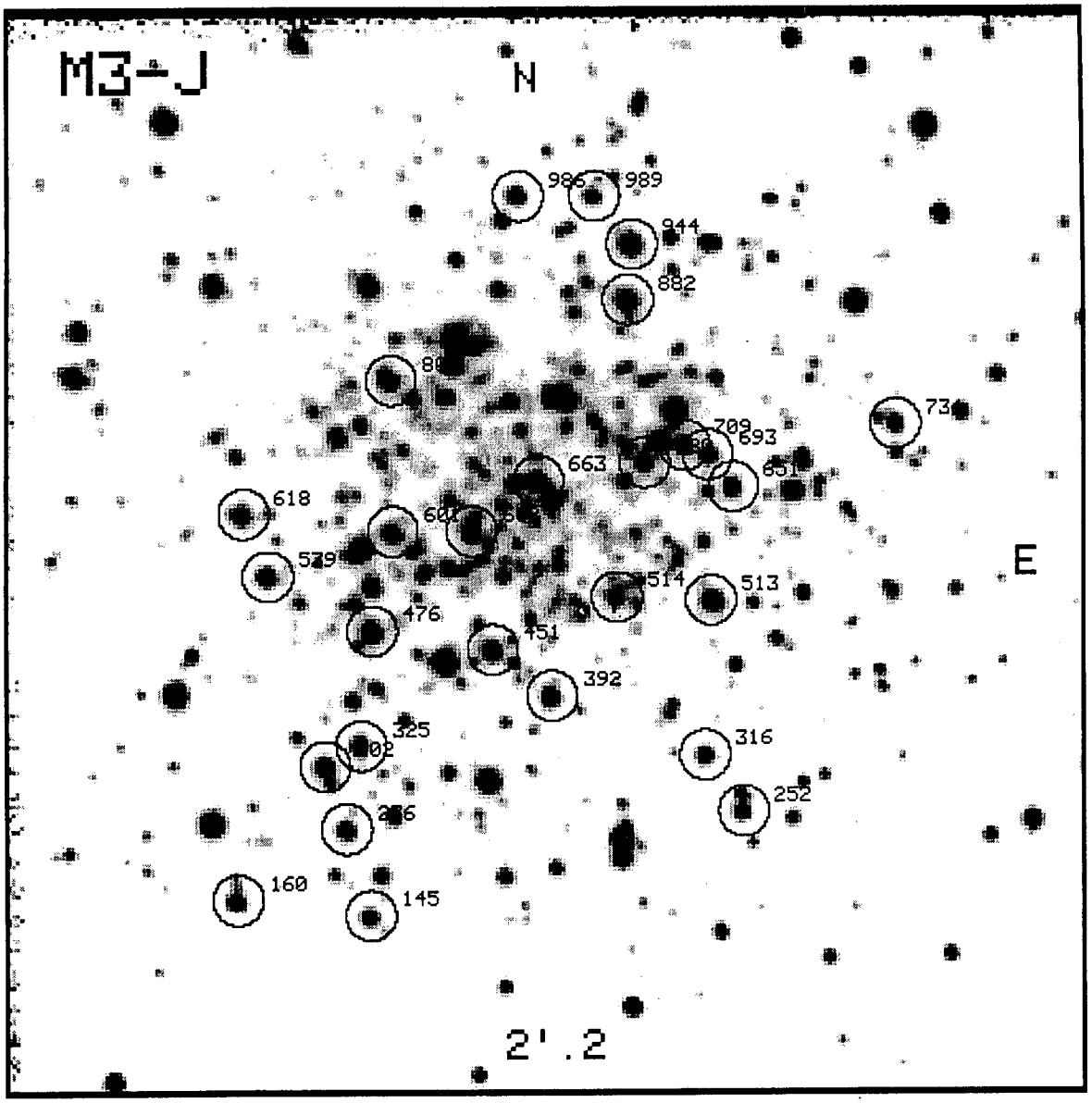

Fig. 1. A greyscale map of the J image of the central region of M3. Circles present the stars brighter than $K \sim 11.5$ magnitude.

in Section IV. Finally the summaries and conclusion follow in Section V.

II. OBSERVATIONS

(a) Observations

Images at J and K bands of M3 were obtained during the observation run of May 12 - 19 in 1995 at Kitt Peak National Observatory(KPNO) with the 2.1m Telescopes equipped with the Cryogenic Optical Bench (COB). COB has a detector type of 256×256 InSb array giving a plate scale of 0.5 seconds per pixel for 2.1m. The field of view covers approximately 2.2×2.2 minutes of arc. The gain of the detector is approximately 6.6 electrons per ADU, and the read noise is 35 electrons.

Because of high background levels in near-infrared observations multiple exposures of each field were obtained and the telescope was offset a few seconds of arcs between these to facilitate the identification and suppression of

Table 1. Journal of observations for M3

Filters	T_{exp}	Air Mass	FWHM(″)
J	20 s	1.02	1″.3
K	20 s	1.09	1″.2

bad pixels and cosmic events.

Dark frames were observed either before or after observations of program objects. Also a series of sky exposures were taken before and/or after each set of cluster observations. A number of standard stars from 'A Set of Faint JHK Standard for UKIRT' (Casali *et al.* 1992) were observed every night during the observation run.

A journal of observation is listed in Table 1 and the final J image of M3 are shown in Figure 1, in which stars brighter than $K \sim 11.5$ mag are marked by circles.

(b) Data Reduction

We reduced the raw image data using the following steps. (1) Bad pixels were detected and fixed in each frame. (2) Dark frames were subtracted from object frames. (3) Sky flat frames were created by combining the dark-subtracted sky frames. (4) Object frames were flattened by using the resulting sky flat frames.

Instrumental magnitudes of the stars in the images were measured by using IRAF/DAOPHOT (Stetson 1987, 1990). The instrumental magnitudes were transformed to the standard system by using the standard stars observed on the same night. Although we observed several standard stars every night of our observing run, it is difficult to reduce the data night by night. Because the extinction coefficients at J and K bands are relatively small, it requires a large number of standard stars to determine them reliably. So we adopted the KPNO standard values for the extinction coefficients: $k_J = 0.06$ and $k_K = 0.04$. We used only the data of the standard stars obtained through the observing run which have small photometric errors to determine the coefficients for the color terms. We used the standard stars brighter than $K = 13$. The final transformation equations we obtained are as follows:

$$J = j + 0.125(\pm 0.008) \cdot (j - k) - 0.060X - 3.496(\pm 0.003), \text{and}$$

$$K = k + 0.013(\pm 0.013) \cdot (j - k) - 0.040X - 4.284(\pm 0.007)$$

In the equations, the lower cases represent the measured instrumental magnitudes, the upper cases represent the standard magnitudes, and X represents an airmass. The fitting errors for the magnitudes and colors are smaller than 0.02 mag.

Finally we have measured the magnitudes and colors of ≈ 200 stars brighter than $K = 14$ mag. JK photometry of the measured stars brighter than $K = 14$ mag in M3 are listed in Table 2. The column (1) gives our catalogue number; the columns (2) and (3) are X and Y positions in pixels which increase to the east and to the north, respectively; the columns (4) and (5) are K and $(J - K)$, respectively. The mean photometric errors, $\sigma(K)$ and $\sigma(J - K)$ along the K magnitudes are listed in Table 3.

III. THE COLOR-MAGNITUDE DIAGRAM

Figure 2 shows the $K - (J - K)$ color-magnitude diagram of $\sim$200 measured stars in M3 which are listed in Table 2. The main feature of these diagrams is the broad red giant branch which shows a rather steep slope. The broadness of the red giant branch is almost entirely due to the photometric errors in our data. The brightest red giant stars in M3 in our images were saturated. Our photometry does not reach the horizontal branch which is fainter than $K = 14$ mag (Guarnieri *et al.* 1990).

We also plotted in Figure 2 the data given by Arribas & Martinez Roger (1987) who presented $UBVRIJHK$ photometry of 24 red giants in M3. They obtained JHK photometry of the red giants using the InSb photometer. The red giants of which they presented JHK photometry are all located outside our imaging field. So we could not compare the photometries of individual stars, but could compare only the general morphology in the CMD

Table 2. JK infrared photometry of the bright stars with $K < 14$ mag in M3

Star	X	Y	K	$(J-K)$	Star	X	Y	K	$(J-K)$
68	118.8	24.9	12.36	0.51	454	186.9	105.6	13.76	0.58
104	148.8	33.7	14.00	0.50	457	83.9	106.1	12.95	0.65
121	170.1	37.8	11.57	0.70	466	120.7	107.4	13.39	0.50
145	86.6	41.5	11.23	0.63	467	183.7	107.6	12.29	0.58
157	123.5	44.5	13.70	0.54	476	87.0	109.3	10.33	0.97
159	151.6	45.1	13.49	0.50	495	183.9	115.0	13.97	0.56
160	55.0	45.3	11.32	0.56	502	83.2	115.8	12.00	0.69
186	54.9	51.0	13.47	0.60	504	178.2	116.2	12.39	0.66
187	118.7	51.2	12.01	0.61	506	70.3	116.3	13.06	0.36
189	89.6	51.6	11.90	0.60	511	131.7	116.6	13.39	0.39
190	78.2	51.8	13.00	0.43	512	135.6	116.7	13.09	0.56
194	33.8	52.7	13.57	0.46	513	167.7	116.7	10.67	0.82
199	131.4	53.3	12.28	0.56	514	145.4	117.5	11.34	0.62
226	178.0	59.2	12.92	0.67	515	98.3	117.5	13.61	0.38
234	33.6	61.1	13.59	0.45	518	189.9	118.5	11.91	0.61
236	80.9	62.1	11.37	0.63	519	124.0	118.6	13.69	0.68
239	112.9	62.9	13.97	0.59	523	109.3	119.2	13.77	0.61
245	187.4	64.8	12.24	0.62	525	226.5	119.4	12.29	0.72
247	92.7	65.2	11.74	0.64	526	147.8	120.0	13.86	0.45
250	112.6	65.8	13.44	0.64	531	150.8	121.4	12.94	0.52
252	175.4	66.2	11.44	0.76	537	144.6	122.0	13.91	0.63
259	59.0	67.6	13.46	0.48	539	62.3	122.5	10.95	0.70
262	146.9	68.2	13.23	0.43	540	118.5	122.7	12.29	0.66
274	175.3	70.4	12.34	0.61	547	100.2	123.9	12.31	0.57
281	96.4	72.4	13.53	0.50	548	109.1	124.0	12.62	0.47
282	77.3	73.0	12.53	0.72	550	127.3	124.4	12.74	0.50
283	189.9	73.2	12.54	0.56	551	105.4	124.6	11.72	0.59
290	195.0	74.9	12.85	0.62	555	132.0	125.1	12.20	0.64
292	90.1	75.3	13.66	0.60	560	74.4	125.8	13.51	0.49
302	75.8	76.9	10.81	0.71	563	119.0	126.2	13.82	0.16
304	40.1	77.3	13.60	0.48	565	113.8	126.6	12.93	0.40
316	166.2	79.6	11.34	0.74	580	115.2	130.4	12.86	0.53
319	159.1	80.2	13.82	0.57	583	121.6	130.6	13.54	0.40
324	27.4	81.8	13.94	0.32	586	165.9	131.1	12.43	0.60
325	84.4	81.8	10.86	0.77	590	64.7	131.6	13.60	0.58
338	69.4	83.9	12.65	0.47	601	92.0	133.3	11.35	0.63
346	125.7	85.8	13.49	0.38	602	110.8	133.4	11.08	0.73
357	119.0	87.9	13.38	0.48	605	173.4	133.8	13.69	0.60
360	95.4	88.3	12.78	0.46	612	126.2	136.1	12.94	0.63
367	158.3	89.1	13.55	0.36	614	79.5	136.4	13.90	0.50
376	136.8	90.8	13.59	0.45	615	201.6	136.9	13.39	0.54
382	158.7	92.1	12.64	0.59	616	130.8	137.2	13.50	0.62
388	82.4	93.0	11.97	0.64	618	56.4	137.5	10.98	0.71
392	130.0	93.8	11.43	0.17	620	62.8	137.9	13.22	0.41
395	32.3	94.6	13.64	0.47	622	178.4	138.0	13.88	0.68
402	88.5	96.0	12.51	0.52	624	123.5	138.1	12.16	0.65
404	208.3	96.2	12.96	0.66	627	200.1	139.1	12.84	0.62
424	202.1	99.1	12.97	0.68	632	118.3	139.7	12.44	0.69
428	207.9	100.1	12.64	0.69	638	105.8	141.1	12.35	0.69
434	174.0	101.4	12.00	0.65	640	80.0	141.8	13.43	0.52
438	216.9	102.0	13.24	0.65	641	181.5	142.0	13.75	0.59
439	121.0	102.0	12.45	0.61	644	133.6	142.5	13.82	0.36
445	44.7	103.8	12.03	0.58	647	166.8	143.1	12.42	0.62
448	98.5	104.0	13.31	0.75	651	173.0	143.9	11.13	0.80
451	115.8	104.9	10.71	0.73	657	121.2	144.9	11.61	0.67
659	156.0	145.4	13.54	0.63	871	148.8	184.5	13.21	0.77
660	193.7	145.4	12.73	0.56	876	135.6	185.9	12.62	0.61
661	147.4	145.5	11.80	0.64	882	147.9	188.8	10.14	0.87
663	126.7	145.5	10.66	0.85	888	161.7	190.3	13.66	0.75
670	197.1	147.1	13.61	0.61	889	134.3	190.6	12.82	0.65

Table 2. (continued)

Star	X	Y	K	$(J-K)$	Star	X	Y	K	$(J-K)$
671	114.1	147.2	13.56	0.40	895	117.3	191.4	12.01	0.70
678	90.3	149.2	13.37	0.66	900	191.4	192.2	13.04	0.67
679	111.5	149.6	12.96	0.67	902	138.6	192.9	12.78	0.56
680	151.9	149.7	11.13	0.75	910	158.7	195.8	12.88	0.53
681	183.4	149.7	12.69	0.70	913	176.9	196.1	13.52	0.51
683	189.9	149.9	11.75	0.71	924	107.4	198.4	12.17	0.67
687	119.8	150.3	13.88	0.72	926	137.3	198.6	13.53	0.76
691	55.2	151.4	12.12	0.64	928	182.8	198.8	12.76	0.67
693	167.0	151.6	11.08	0.81	934	54.0	200.1	13.49	0.54
697	211.8	152.1	12.09	0.75	944	148.9	202.0	10.25	0.73
700	218.7	152.3	13.42	0.71	945	175.9	202.1	13.30	0.73
703	94.8	152.8	12.94	0.60	951	158.2	203.5	11.97	0.63
708	148.1	153.8	12.22	0.71	957	132.6	204.9	13.05	0.71
709	161.4	153.9	10.98	0.74	959	134.9	206.0	13.02	0.66
716	142.1	154.7	13.61	0.50	965	118.2	207.7	11.71	0.76
722	78.9	156.0	11.59	0.63	972	98.1	209.8	12.43	0.58
725	142.7	157.0	13.57	0.68	976	188.3	211.3	13.36	0.63
726	111.0	157.1	13.49	0.52	981	182.4	212.9	12.07	0.76
728	122.6	157.5	12.78	0.47	986	122.0	213.6	10.93	1.29
732	186.5	158.6	13.49	0.62	989	140.2	213.6	11.50	0.73
733	84.5	158.8	11.69	0.71	995	150.6	214.7	13.82	0.46
734	211.7	158.9	11.32	0.80	1002	189.9	215.7	13.09	0.78
739	140.4	159.6	12.34	0.61	1012	141.4	217.9	13.73	0.72
743	207.4	160.4	12.55	0.69	1016	145.3	218.5	13.12	0.52
751	227.8	161.8	11.51	0.78	1024	36.7	220.4	13.18	0.51
753	73.3	162.0	12.74	0.57	1032	153.8	222.3	12.92	0.71
755	115.2	162.8	13.76	0.71	1034	98.7	222.6	13.95	0.64
769	120.1	164.5	11.84	0.61	1042	129.6	224.4	13.09	0.67
774	129.7	164.9	12.03	0.58	1052	137.4	227.0	13.41	0.73
776	97.1	165.0	11.87	0.71	1053	145.0	227.0	13.62	0.50
792	82.2	168.5	13.53	0.49	1059	147.0	228.7	13.60	0.53
800	153.4	169.4	13.14	0.46	1065	144.8	230.9	13.77	0.55
801	91.5	169.4	10.75	0.76	1069	98.8	232.5	13.91	0.61
802	191.5	169.8	13.03	0.64	1077	150.8	234.7	11.93	0.79
804	205.3	170.4	13.98	0.29	1082	26.7	236.2	13.08	0.58
808	162.9	171.3	12.43	0.67	1088	151.6	237.3	12.45	0.75
811	136.6	171.9	12.55	0.69	1108	35.7	245.1	13.44	0.56
833	183.6	176.8	13.92	0.63	1112	119.5	248.4	12.51	0.62
837	100.9	179.2	13.59	0.81	1115	59.6	249.1	13.69	0.38
843	93.0	179.7	13.34	0.51	1116	162.4	249.5	13.43	0.77
856	146.6	181.7	13.06	0.63					

Table 3. Mean photometric errors versus K

K	$\sigma(K)$	$\sigma(J-K)$
11.5	0.02	0.03
12.0	0.02	0.03
12.5	0.03	0.04
13.0	0.03	0.04
13.5	0.04	0.06
14.0	0.06	0.09

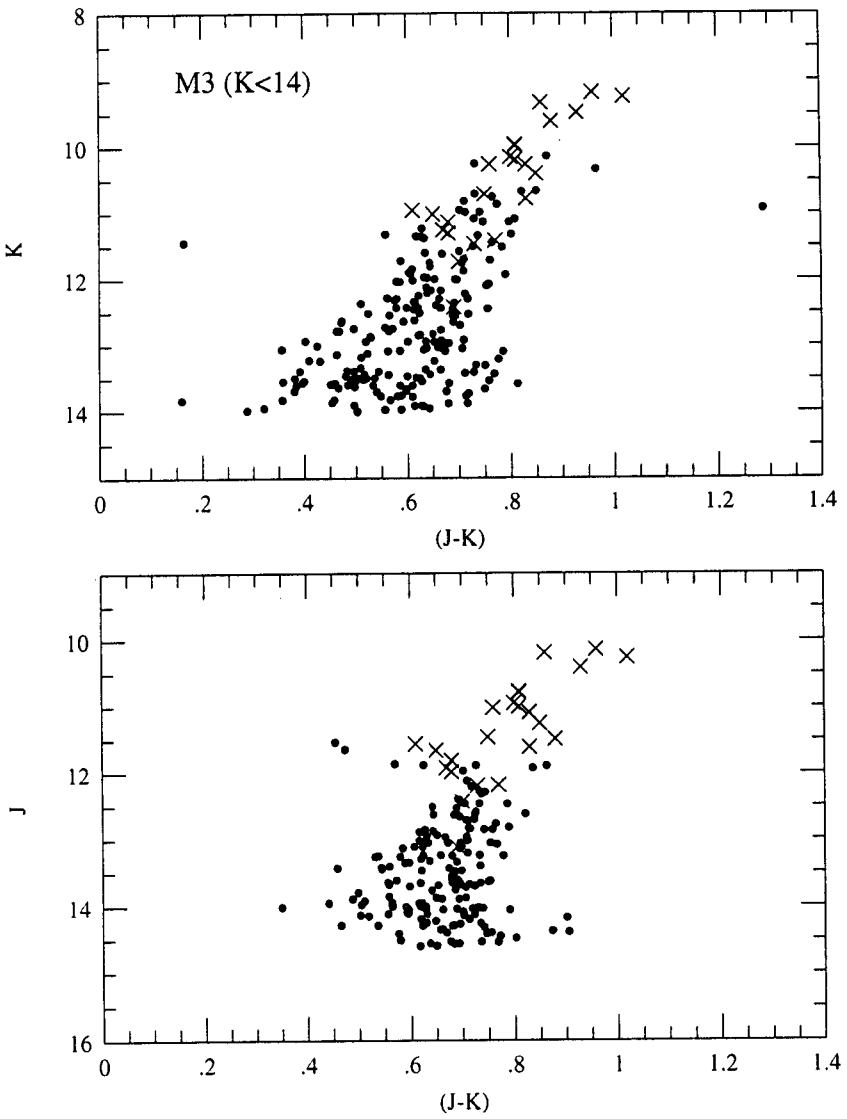

Fig. 2. Infrared color-magnitude diagrams for the bright stars in the central region of M3. Upper panel: K-$(J-K)$ CMD; Lower panel: J-$(J-K)$ CMD. The filled circles and the crosses represent the photometries of this study and Arribas & Martinez Roger (1987), respectively.

of theirs and ours. Figure 2 shows that the upper part of the red giant branch of our data agree well with the lower part of the red giant branch given by Arribas & Martinez Roger. The normal points of the red giant branch of M3 were derived from the original data up to $K = 15$ by sorting the observations into bins of width 0.5 mag at K magnitudes and calculating the mean of $(J-K)$ distribution in each bin. The results are listed in Table 4. The uncertainties in the normal points, the rms deviation of the mean of $(J-K)$, were computed from the $(J-K)$ distribution in each magnitude bin. The uncertainty, $\sigma(J-K)$, increases toward fainter magnitudes from 0.05 at $K = 10.75$ mag to 0.22 at $K = 14.75$ mag.

The separation between the red giant branch and asymptotic giant branch (AGB) which is seen in CMDs of the optical region is not seen in these IR CMDs. The gap in giant branch found at $V = 13.4$ mag and $(B-V) = 1.15$ by Sandage & Katem (1982) is not distinctive at these CMDs either. Because most of the brightest giants were saturated on the 20 sec exposure frames, there are not many stars brighter than $K = 11$, to make certain of the gap. If we adopt the relation between $(B-V)$ and $(J-K)$ of giants which was derived from the

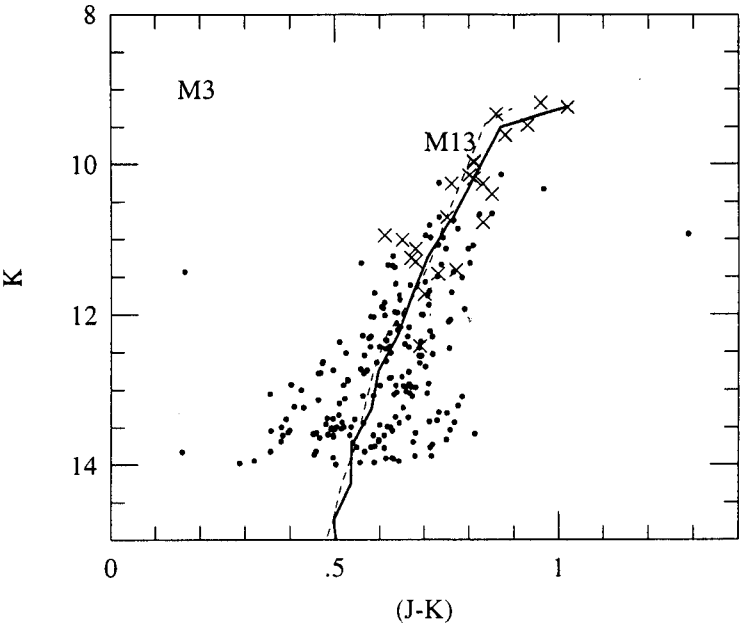

Fig. 3. Comparison of the red giant branches of M3 and M13 in the K-$(J-K)$ CMD. The filled circles and crosses represent, respectively, the photometries of this study and Arribas & Martinez Roger (1987). The solid line and the dashed line represent the mean loci of the red giant branches of M3 and M13, respectively.

study of M13 by Davidge *et al.* (1995), the gap is expected to be located around $K = 10.5$ mag and $(J-K) = 0.72$ for M3. The color-magnitude diagram of K vs $(J-K)$ in Figure 2 shows that only 3 stars are brighter than $K = 10.5$ mag with only hints for some possibility of a gap around it. In order to make sure of it, we have to wait until more data are collected.

Table 4. Mean locus of the red giant branch of M3

K	$(J-K)$	$\sigma(J-K)$
10.75	0.76	0.05
11.25	0.71	0.08
11.75	0.67	0.06
12.25	0.64	0.06
12.75	0.60	0.09
13.25	0.58	0.12
13.75	0.54	0.13
14.25	0.54	0.16
14.75	0.50	0.22

IV. COMPARISON WITH OTHER CLUSTERS

Although many parameters of M3 have been determined quite agreeably, the situation for the metallicity appears to be rather different. Previous estimates for the mean metallicity of M3 vary from [Fe/H] = −1.32(Bica & Pastoriza 1983), −1.47(Frogel *et al.* 1983; Kraft *et al.* 1992), −1.49(Geisler 1984), −1.57(Smith 1984), −1.43(Pilachowski 1984), to −1.66(Zinn & West 1984; Buonanno *et al.* 1994). The discrepancy between the high resolution spectroscopic result of Kraft *et al.* (1992), which was based on seven giants of M3, and the mean metallicity computed by Zinn & West (1984), who used a variety of metallicity indicators, is 0.19 dex.

Therefore, we have intended to get some information for the mean metallicity of M3 that would be quite free from any assumptions, by using direct comparisons with CMDs of other clusters.

M13 is a very bright globular cluster which has been a target of many studies, and the metallicity of M13 is known to be very similar to that of M3 from various methods. Since infrared CMDs of M13 (Davidge *et al.* 1995) are available, we have compared them with the result of this study to get a better information of the metallicity of M3. Figure 3 displays a comparison of M3 and M13 in the K–$(J-K)$ CMD.

The difference of the distance moduli at K-band between M3 and M13, $\delta(\mathrm{m}-\mathrm{M})_K = 0.76$, is applied to the plot of the red giant branch mean loci of those clusters in Figure 3. We have found that there is an almost exact match between RGBs of M3 and M13. It implies that the metallicity of M3 is quite similar to that of M13. If we adopt the metallicity of [Fe/H]= −1.6 by Davidge *et al.* (1995) for M13, we could say that the metallicity of M3 is close to −1.6.

However, for M13 metallicity, a discrepancy of 0.14 dex is also found between the high resolution spectroscopic result of Kraft *et al.* (1992), which was based on 13 giants, and the mean metallicity from a variety of metallicity indicator by Zinn & West(1984). We can conclude that we have confirmed that metallicities of M3 and M13 are almost the same.

V. SUMMARY AND CONCLUSION

We have presented new photometric data at J and K bands of ≈200 red giant stars brighter than $K = 14$ mag in the central $2'.2 \times 2'.2$ region of the globular cluster M3. The infrared CMDs of M3 from these data show a steep red giant branch.

The CMD of M3 has been compared with that of M13. After correcting for the differences in the distance, the mean locus of the red giant branch in M3 is found to be very similar to that of M13. This result shows that the both M3 and M13 clusters have almost the same metallicity.

ACKNOWLEDGEMENT

This work was supported in part by the Basic Science Research Institute Program, Ministry of Education, Korea, BSRI-95-5411.

REFERENCES

Arribas, S. & Martinez Roger, C. 1987, A&A, 178, 106
Auriere, M. & Cordoni, J. P. 1983, A&AS, 52, 383
Bica, E. D. L. & Pastoriza, M. G. 1983, AP&SS, 91, 99
Buonanno, R., Buzzoni, A., Corsi, C. E., Fusi-Pecci, F. & Sandage, A. R. 1986, Mem. Sco. Astron. It, 57, 391
Buonanno, R., Corsi, C. E., Bussoni, A., Cacciari, C., Ferraro, F. R. & Fusi-Pecci, F. 1994, A&A, 290, 68
Buonanno, R., Corsi, C. E. & Fusi-Pecci, F. 1989, A&A, 216, 80
Burgarella, D., Paresce, F. & Quilichini, V. 1995, A&A, 301, 675
Burstein, D. & McDonald, L. H. 1975, AJ, 80, 17
Casali, M. & Hawarden, T. 1992, The JCMT–UKIRT NEWSLETTER, Number 4, August 1992, p 33
Cohen, J. G., Frogel, J. A., & Persson, S. E. 1978, ApJ, 222, 165
Davidge, T. J. & Harris, W. E. 1995, ApJ, 445, 211
——— 1996, ApJ, 462, 255
Davidge, T. J. & Simons, D. A. 1994, ApJ, 423, 640
Frogel, J. A., Persson, S. E. & Cohen, J. G. 1983, ApJS, 53, 713
Geisler, D. 1984, ApJ, 287, L85
Guarnieri, M. D., Longmore, A. J., Fusi-Pecci, F. & Dixon, R. I. 1990, Mem. Soc. Astron. Ital, 61, 143
Guhathakurta, P., Yanny, B., Bahcall, J. N. & Schneider, D. P. 1994, AJ, 108, 1786
Houdashelt, M. L., Frogel, J. A., & Cohen, J. G. 1992, AJ, 103, 163

Kraft, r. P., Sneden, C., Langer, G. E. & Prosper, C. F. 1992, AJ, 104, 645
Paez, E., Roger, M. C. & Straniero, O. 1990, AP&SS, 169, 15
Paez, E., Straniero, O. & Roger M. C. 1990, A&AS, 84, 481
Phillips, J. P., Roger, M. C., Magro, S. C. & Vilchez, L. 1986, A&A, 161, 257
Pilachowski, C. A. 1984, ApJ, 281, 614
Rieke, G. H. & Lebofsky, M. J. 1985, ApJ, 288, 618
Sandage, A. 1953, AJ, 58, 61
——— 1970, ApJ, 162, 841
Sandage, A. & Katem, B. 1982, AJ, 87, 537
Smith, H. A. 1984, ApJ, 281, 148
Stetson, P. B. 1987, PASP, 99, 191
———— 1990, PASP, 102, 932
Stetson, P. B. & Harris, W. E. 1988, AJ, 96, 909
Zinn, R. J. & West, M. J. 1984, ApJS, 55, 45